nature medicine

mTOR inhibition reverses Akt-dependent prostate intraepithelial neoplasia through regulation of apoptotic and HIF-1-dependent pathways

Pradip K Majumder[1,2], Phillip G Febbo[1,2], Rachel Bikoff[1,2], Raanan Berger[1,2], Qi Xue[1,2], Louis M McMahon[3], Judith Manola[1], James Brugarolas[1,2], Timothy J McDonnell[4], Todd R Golub[1,2,5], Massimo Loda[1,2], Heidi A Lane[6] & William R Sellers[1,2,5]

Loss of PTEN function leads to activation of phosphoinositide 3-kinase (PI3K) signaling and Akt. Clinical trials are now testing whether mammalian target of rapamycin (mTOR) inhibition is useful in treating PTEN-null cancers. Here, we report that mTOR inhibition induced apoptosis of epithelial cells and the complete reversal of a neoplastic phenotype in the prostate of mice expressing human *AKT1* in the ventral prostate. Induction of cell death required the mitochondrial pathway, as prostate-specific coexpression of *BCL2* blocked apoptosis. Thus, there is an mTOR-dependent survival signal required downstream of Akt. Bcl2 expression, however, only partially restored intraluminal cell growth in the setting of mTOR inhibition. Expression profiling showed that Hif-1α targets, including genes encoding most glycolytic enzymes, constituted the dominant transcriptional response to AKT activation and mTOR inhibition. These data suggest that the expansion of AKT-driven prostate epithelial cells requires mTOR-dependent survival signaling and activation of HIF-1α, and that clinical resistance to mTOR inhibitors may emerge through BCL2 expression and/or upregulation of HIF-1α activity.

© 2004 Nature Publishing Group http://www.nature.com/naturemedicine

Inactivation of the tumor-suppressor gene *PTEN* occurs in glioblastoma multiforme, endometrial cancer and prostate cancer, among others. The tumor-suppressor function of PTEN is linked to its lipid phosphatase activity; loss of this activity leads to accumulation of its substrate, phosphatidylinositol 3,4,5-trisphosphate, and activation of the PI3K signaling pathway[1]. One consequence of PTEN loss is hyperactivation of the oncogenic serine/threonine kinase AKT and phosphorylation of downstream AKT substrates, including BAD[2], FOXO proteins[3,4] and GSK3 (ref. 5). Phosphorylation and inactivation of these proteins can lead to enhanced cell survival, increased cell proliferation and altered cellular metabolism. PI3K signaling has been implicated in the regulation of mTOR (in mouse, encoded by the gene *Frap1*) and S6K. In *Drosophila melanogaster*, loss of *Tor* is epistatic to loss of *Pten*, and in mouse and cell-based models loss of PTEN sensitizes cells to mTOR inhibition[6–10]. This pathway has been further elucidated through studies in *D. melanogaster* and mammalian cells showing that tuberin, the protein product of *Tsc2*, regulates *Tor* and is an AKT substrate. Thus, AKT-dependent phosphorylation inhibits tuberin, leading to activation of mTOR and S6K[11–15]. On the basis of these cumulative observations, derivatives of the mTOR inhibitor rapamycin are being tested in clinical trials in patients with cancer[16].

We previously showed that a probasin promoter-myr-HA-*AKT1* transgene directs production of activated AKT1 spatially restricted to the luminal epithelial cells of the mouse ventral prostrate and, as a result, these mice develop a highly penetrant prostatic intraepithelial neoplasia (PIN) phenotype[17]. The phenotype bears many of the hallmarks of mTOR activation including increased cell number, increased cell size, and activation of the downstream kinase S6K, together suggesting that activation of mTOR downstream of AKT may be linked to the development of PIN in these mice. Here, we show that the Akt-induced PIN phenotype is completely dependent on mTOR. Specifically, treatment with the mTOR inhibitor RAD001 led to a rapid loss of intraluminal epithelial cells marked by the induction of apoptosis, and reversed the PIN phenotype within 14 d. Mice carrying both *AKT1* and *BCL2* transgenes were resistant to RAD001-induced apoptosis and had a PIN phenotype partially resistant to RAD001. Further analysis of this partial resistance showed that Hif-1α target genes, including those encoding enzymes essential for glycolysis, were the principal constituents of the transcriptional response to elevated Akt activity and of the response to mTOR inhibition. These data suggest that the response to mTOR inhibition is mediated through independent apoptotic and Hif-1α regulatory pathways.

[1]Departments of Medical Oncology, Pediatric Oncology and Biostatistical Sciences, Dana-Farber Cancer Institute, 44 Binney Street, Boston, Massachusetts 02115, USA. [2]Departments of Medicine and Pathology, Brigham and Women's Hospital, Harvard Medical School, 75 Francis Street, Boston, Massachusetts 02115, USA. [3]Novartis Pharmaceutical Corporation, One Health Plaza, East Hanover, New Jersey 07936, USA. [4]Department of Molecular Pathology, The University of Texas M.D. Anderson Cancer Center, Houston, Texas 77030, USA. [5]The Broad Institute at Harvard and MIT, 320 Charles Street, Cambridge, Massachusetts 02142, USA. [6]Novartis Institute for Biomedical Research, Oncology, CH-4002 Basel, Switzerland. Correspondence should be addressed to W.R.S. (william_sellers@dfci.harvard.edu).

Published online 23 May 2004; doi:10.1038/nm1052

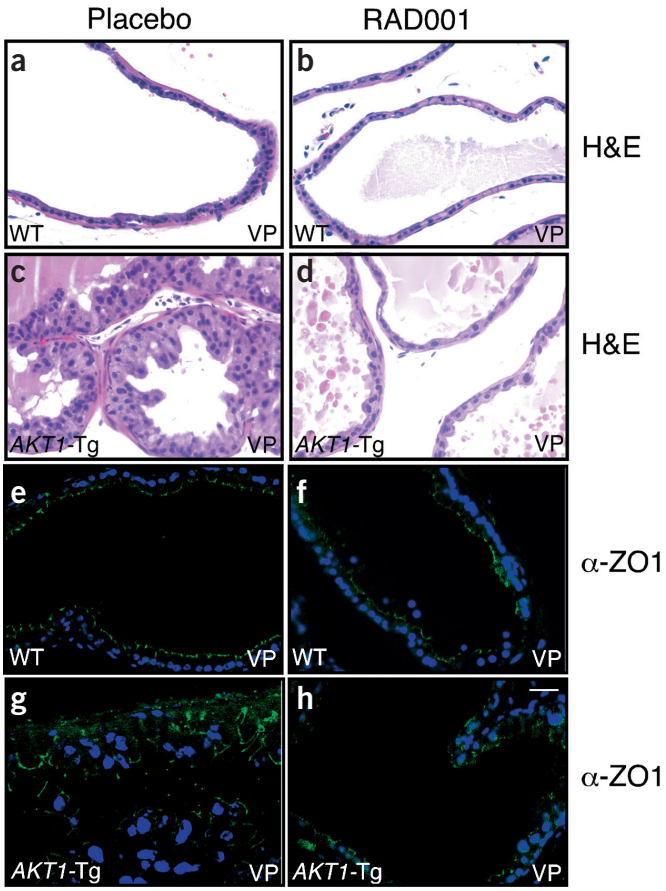

Figure 1 An mTOR inhibitor (RAD001) reverses the PIN phenotype of *AKT1*-Tg mice. (**a**–**h**) Wild-type (WT) (**a**,**b**,**e**,**f**) and *AKT1*-Tg mice (**c**,**d**,**g**,**h**) were treated for 14 d with either placebo (**a**,**c**,**e**,**g**) or 10 mg/kg/d RAD001 (**b**,**d**,**f**,**h**). Shown are H&E-stained tissue sections from ventral prostate (VP) harvested from both untreated (**a**,**c**) and treated mice (**b**,**d**). Data are representative of 12 mice in each treatment group. Tissue sections from both control and RAD001-treated mice were stained with antibody to Zo1 (α-Zo1) and imaged by confocal microscopy (**e**–**h**). Scale bar, 25 μm.

RESULTS

Reversal of AKT-dependent PIN by mTOR inhibition

To determine whether an Akt1-induced PIN phenotype requires mTOR activity, 8- to 12-week-old transgenic mice expressing human *AKT1* in the ventral prostate (*AKT1*-Tg) and wild-type mice were treated with placebo or the mTOR inhibitor RAD001 (everolimus), an orally active rapamycin derivative[18]. At this age the PIN phenotype is fully developed in all *AKT1*-Tg mice[17]. Peak and trough concentrations for blood and for ventral prostate exceeded the concentration producing 50% growth inhibition (IC_{50}) of human tumor cell lines deemed sensitive to RAD001 (**Supplementary Fig. 1** online; H.A.L. and T. O'Reilly, unpublished data), and at 10 mg/kg/d, RAD001 was well tolerated with no change in body weight (**Supplementary Fig. 1** online).

After 14 d the ventral prostate histology of placebo or RAD001-treated wild-type mice was normal, whereas PIN persisted in *AKT1*-Tg mice treated with placebo. However, treatment of *AKT1*-Tg mice with RAD001 restored cell size, epithelial cell polarization (measured by ZO-1 staining) and the luminal architecture to normal (**Fig. 1a–h** and **Supplementary Figs. 2** and **3** online). Most notably, the ductal lumens were now devoid of the excessive cells seen in placebo-treated *AKT1*-Tg mice. These data suggest that the genesis and/or survival of the intraluminal cells driven by Akt expression is mTOR dependent.

Phenotype regression despite continued AKT activity

To determine whether RAD001 selectively inhibited mTOR without altering other elements of Akt signaling, tissue sections and protein extracts were probed with antisera recognizing phosphorylated Ser235/236 on S6RP and phosphorylated Ser1108 on eIF4G. The latter is both serum dependent and inhibited by rapamycin[19]. Phosphorylation of S6RP and eIF4G was elevated in *AKT1*-Tg mice as compared with control mice, and was reduced by RAD001 (**Fig. 2a–d,i**).

Next, we examined the phosphorylation of Akt and GSK3, a well-defined Akt substrate. In *AKT1*-Tg mice, RAD001 had no effect on the elevated levels of pS473-Akt or pS9/21-GSK3 compared with placebo-treated controls (**Fig. 2e–i**), suggesting that in these mice RAD001 acts selectively downstream of AKT to inhibit mTOR activity. Thus, the AKT-induced PIN phenotype is mTOR dependent.

An mTOR-dependent survival pathway

To determine the time course of the response to RAD001, we treated 228 *AKT1*-Tg and wild-type mice for 6 h, 12 h, or with daily dosing for 1 d, 2 d, 3 d, 9 d and 14 d with either RAD001 or placebo (**Fig. 3**). No histologic changes were noted through 3 d of RAD001 treatment, but on day 9 luminal cells appeared vacuolated and were reduced in number. At this time there was also an increase in intraluminal cellular debris followed by complete clearing of the lumens by day 14.

In the ventral prostate of *AKT1*-Tg mice, the rate of cellular proliferation (measured by 5-bromodeoxyuridine (BrdU) incorporation) was only modestly elevated compared with wild-type controls and, as anticipated, is reduced by RAD001 (**Supplementary Fig. 4a–e** online). The lack of large numbers of proliferating cells, the cytopathic changes seen at day 9 and the rapidity of the phenotypic reversion suggested that loss of intraluminal cells after RAD001 exposure might be due to programmed cell death. In support of this idea, DNA fragmentation, measured by fluorescent TdT-mediated dUTP nick end labeling (TUNEL) at 6 h, 12 h, 24 h and 48 h after RAD001 initiation, showed a substantially higher percentage of apoptotic cells after 48 h than did placebo controls (**Fig. 4a–h,m**). Additional experiments over longer treatment periods showed a continued increase in the number of apoptotic cells while the extent of proliferation inhibition remained constant (**Fig. 4n**). In parallel, caspase-3 activation, measured by immunostaining, was detected within 24 h of RAD001 treatment (**Fig. 4i–l**). These data suggest that the intraluminal epithelial cells contributing to the PIN phenotype depend on an mTOR-dependent, antiapoptotic signaling pathway for their continued survival, and that the consequences of mTOR inhibition in reversing the AKT phenotype arise, at least in part, from proapoptotic effects.

Apoptosis induced by mTOR inhibition is blocked by BCL2

To determine whether apoptosis induced by mTOR inhibition required mitochondrial pathway activation, *AKT1*-Tg mice were intercrossed with transgenic mice expressing *BCL2* specifically in the ventral prostate (*BCL2*-Tg)[20]. We treated ten mice of each genotype from this intercross with RAD001 or placebo for 14 d. Consistent with the results obtained in *AKT1*-Tg mice, RAD001 fully reversed the PIN in F1 mice bearing only the *AKT1* transgene. In contrast, in mice carrying both *AKT1*-Tg and *BCL2*-Tg, RAD001 administration

© 2004 Nature Publishing Group http://www.nature.com/naturemedicine

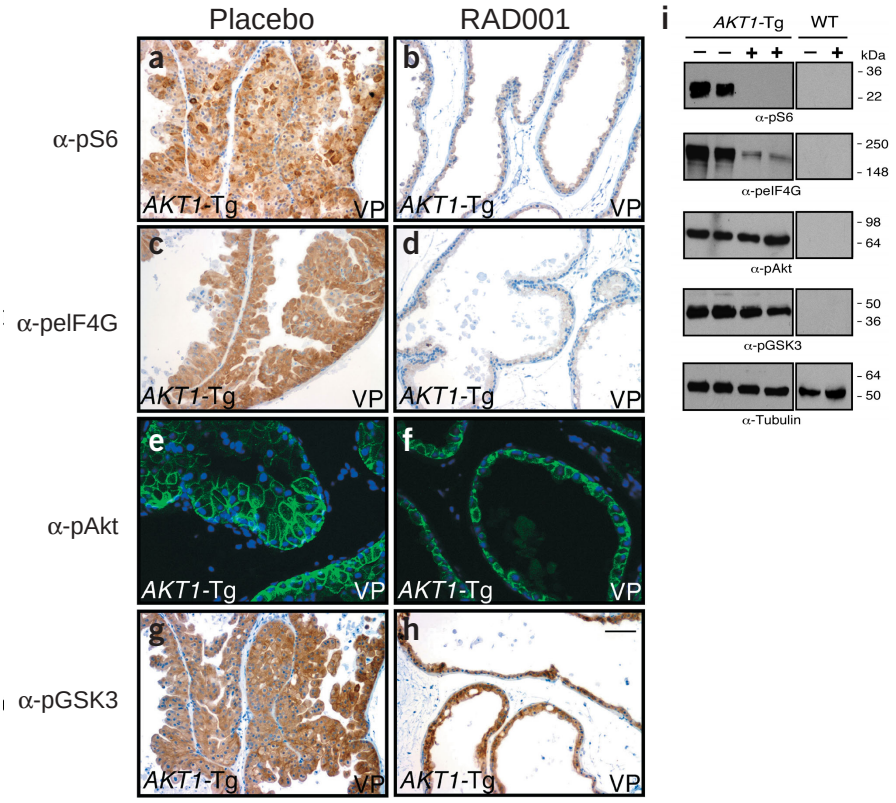

Figure 2 Selective *in vivo* inactivation of mTOR and S6K activity by RAD001. (**a**–**h**) *AKT1*-Tg mice were treated with placebo (**a**,**c**,**e**,**g**) or RAD001 (**b**,**d**,**f**,**h**) for 14 d, and ventral prostate sections were probed with antibodies to pS6RP (**a**,**b**), peIF4G (**c**,**d**), pAKT (**e**,**f**) or pGSK3 (**g**,**h**). The data are representative of results obtained in 12 mice per treatment group. Scale bar, **a**–**d**,**g**,**h**, 50 μm; **e**,**f**, 25 μm. (**i**) Protein lysates from the ventral prostate of *AKT1*-Tg and wild-type mice treated with RAD001 (+) or placebo (–) for 72 h were subject to immunoblot analysis with antibodies to pS6RP, peIF4G, pAKT, pGSK3 or tubulin as indicated.

completely inhibited mTOR signaling, but partial rather than complete regression of the phenotype occurred (**Fig. 5a-h** and **Supplementary Fig. 5** online). Inhibition of mTOR suppressed proliferation in both wild-type *AKT1* and *AKT1*-Tg/*BCL2*-Tg mice (**Supplementary Fig. 5** online), whereas TUNEL staining after 48 h showed that RAD001 induced an increase in apoptotic cells in wild-type *Akt1* mice, but no change in apoptosis in *AKT1*-Tg/*BCL2*-Tg mice (**Supplementary Fig. 5** online). Thus, BCL2 expression blocked the induction of apoptosis by mTOR inhibition and led to partial phenotype resistance to RAD001.

mTOR-dependent regulation of Hif-1α target genes

Although expression of BCL2 blocked RAD001-induced apoptosis, the PIN phenotype was only partially restored. Specifically, in the compound transgenic mice treated with RAD001, PIN consisting of two to three epithelial cell layers was seen, but more extensive luminal filling, as seen in untreated mice, was not observed. Thus, to further understand the pathways mediating the expansion of the intraluminal cells and the response to RAD001, we carried out expression profiling followed by gene-set enrichment analysis (GSEA)[21].

First, total RNA was prepared after 12 or 48 h of RAD001 or placebo treatment in wild-type and *AKT1*-Tg mice, and message abundance was determined for ~22,626 genes using microarrays. To identify genes altered by AKT expression and by subsequent mTOR inhibition, artificial values for gene expression representing an idealized response to AKT expression and mTOR inhibition were set, and the correlation between these values and the actual expression data was determined using the Pearson coefficient. There were 654 features (representing 571 unique genes or expressed sequence tags) with significant correlation to this vector (**Supplementary Table 1** online; $P \leq 0.001$).

To determine whether the differential expression of this set of genes resulted from alterations in the activity of specific molecular pathways, we applied GSEA to this data set[21]. We identified defined gene sets having statistically significant increased or decreased coordinate gene expression between two experimental conditions. We tested 192 previously specified Biocarta gene sets in GSEA by comparing *AKT1*-Tg samples treated with RAD001 ($n = 9$) or placebo ($n = 10$). Gene sets that achieved enrichment greater than expected

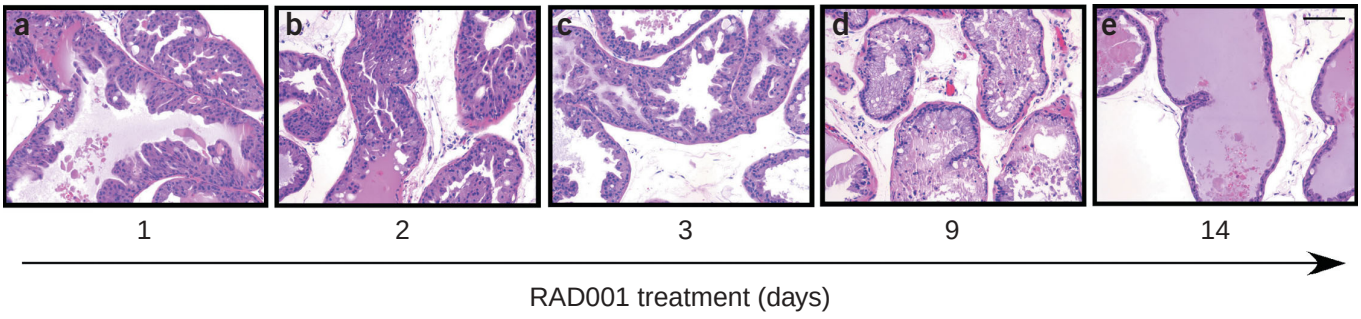

Figure 3 Time course of the phenotypic response to mTOR inhibition. (**a**–**e**) *AKT1*-Tg mice were treated with 10 mg/kg/d of RAD001 for 1, 2, 3, 9 and 14 d. Tissue sections from the ventral prostate were stained with H&E. Shown are sections representative of the results obtained in at least 12 mice evaluated after each specific treatment period. Scale bar, 50 μm.

© 2004 Nature Publishing Group http://www.nature.com/naturemedicine

© 2004 Nature Publishing Group http://www.nature.com/naturemedicine

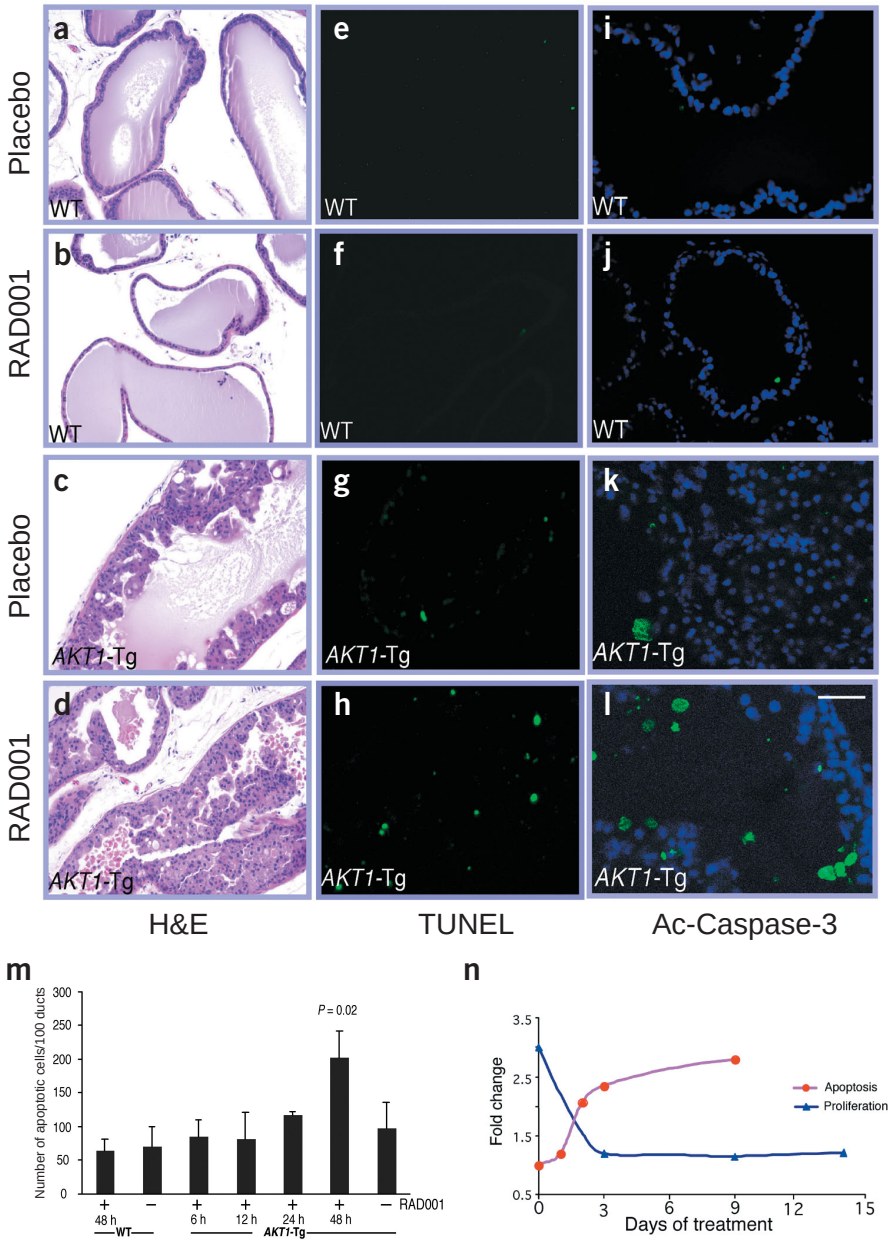

Figure 4 Induction of cell death by mTOR inhibition in *AKT1*-Tg mice. (**a**–**h**) H&E (**a**–**d**) or TUNEL staining (**e**–**h**) of wild-type (**a**,**b**,**e**,**f**) and *AKT1*-Tg mice (**c**,**d**,**g**,**h**) treated with placebo (**a**,**c**,**e**,**g**) or RAD001 (**b**,**d**,**f**,**h**) for 48 h. (**i**–**l**) Caspase-3 activation was assessed in wild-type (**i**,**j**) and *AKT1*-Tg mice (**k**,**l**) treated with placebo (**i**,**k**) or RAD001 (**j**,**l**) for 24 h. All results are representative of those obtained in six mice. (**m**) TUNEL-positive cells (mean ± s.e.m. per 100 ducts after RAD001 (+) or placebo (–). (**n**) Mean fold change (RAD001 versus placebo) in the apoptotic or proliferation index for at least three *AKT1*-Tg mice at each time point. Scale bar, **a**–**h**, 50 μm; **i**–**l**, 25 μm.

by chance alone were identified by permuting the placebo and RAD001 sample labels. In this analysis, a seven-member, hypoxia-inducible factor 1 gene set that included *Vegfa*, *Edn1* (endothelin-1), *Ldh1* (lactate dehydrogenase-1) and *Hif1a* (Hif-1α) was the only set to have a validation mode significance less than 0.05 (**Fig. 6a**). To further explore this finding, GSEA was carried out using a list independently curated from the literature of putative Hif-1α transcriptional target genes[22]. This analysis showed marked enrichment for the expression of Hif-1α target genes in *AKT1*-Tg as compared to wild-type mice and a statistically significant collective loss of expression of Hif-1α transcriptional targets in RAD001- versus placebo-treated mice (**Fig. 6b** and **Supplementary Fig. 6** online). This set of Hif-1α target genes includes *Slc2a1* (Glut1), *Vegfa*, *Hmox1* (heme oxygenase-1) and *Apba2bp* (NIP3); however, most prominently enriched in this set were genes encoding enzymes comprising the glycolysis pathway (**Fig. 6b**,**c**). Indeed, 9 of 10 genes encoding enzymes involved in the conversion of glucose to pyruvate were among the top genes in this set and were strongly upregulated in the *Akt1*-Tg mouse and downregulated by RAD001 within 12 h and 48 h (**Fig. 6c**). In addition, lactate dehydrogenase, which under anaerobic conditions converts pyruvic acid to lactic acid, was regulated in a similar manner (**Fig. 6c**). Moreover, the glycolytic enzymes as an independent gene set were fourth among pathways ranked by GSEA (**Fig. 6a**) and coclustered when these data were analyzed by unsupervised hierarchical clustering (data not shown).

These data suggest that Hif-1α activity is upregulated in the AKT transgenic animals and downregulated after RAD001 administration. To independently validate these results, Glut1 was detected in tissue sections by immunohistochemistry and was significantly downregulated by RAD001 (14 d) in both *AKT1*-Tg and *AKT1*-Tg/*BCL2*-Tg prostates (**Fig. 6d**). In keeping with the indirect measures of Hif-1α activity, immunoblot analysis showed marked upregulation of the Hif-1α protein in extracts prepared from the ventral prostates of *AKT1*-Tg/*BCL2*-Tg mice, which was reduced to basal levels after three doses of RAD001. These alterations in Hif-1α protein were paralleled by changes in Hif-1α mRNA (**Fig. 6e**). Thus, it seems likely that mTOR activity leads to changes in both mRNA and protein for Hif-1α.

These data suggest that, in this model of AKT activation, mTOR inhibition leads to independent activation of apoptotic pathways and inactivation of Hif-1α target genes.

DISCUSSION

Many genetic alterations, including loss of *PTEN*[23], mutation of the gene encoding phosphoinositide 3-kinase p110α (*PIK3CA*[24]), amplification of *PIK3CA*[25] and amplification of *AKT1* and *AKT2*, can lead to activation of AKT kinase activity[23]. Here, we show that an AKT-induced PIN phenotype is completely mTOR dependent. Of note, AKT induces this dependency in normal prostate epithelial cells that evidently have no dependence on mTOR. The phenotype reversion

© 2004 Nature Publishing Group http://www.nature.com/naturemedicine

seen with mTOR inhibition is in part due to the induction of apoptosis within the intraluminal cells. Thus, these intraluminal cells, and not the cells localized along the basement membrane (which continue to harbor activated AKT), become dependent on continuous mTOR activity. This specific sensitivity of the luminal cells recalls the selective regulation of luminal apoptosis seen in three-dimensional models of immortalized mammary epithelial cells[26], in which Akt-driven proliferation is also dependent on mTOR[27], and suggests that loss of luminal cell interactions with the matrix or with basal epithelial cells or the loss of endogenous survival factors has a role in rendering cells mTOR dependent for survival.

Pten$^{+/-}$ mice, human xenografts and transformed chicken fibroblasts are sensitive to mTOR inhibition[8–10]. Whereas in such settings mTOR inhibition is primarily cytostatic, in the *AKT1*-Tg model there is clear phenotype reversion. Several possibilities might explain these differences. First, selective activation of AKT rather than loss of PTEN may render cells dependent on mTOR rather than on mTOR together with additional pathways. Second, the PIN phenotype is not invasive. As the effects of mTOR inhibition were most profound within the intraluminal cells, it is possible that, as cells invade through the basement membrane, they gain new survival signals (or regain the basal survival signals)—rendering them mTOR independent for survival. Indeed, data published while this work was in progress demonstrated that Akt-driven lymphomas treated with rapamycin, although partially responsive, rarely achieved complete responses, although combination with doxorubicin led to far greater antilymphoma activity than that for either agent alone[28]. Third, cell lines and xenografts reflect a more complex genetic background than the *AKT1*-Tg model. Thus, it is possible that other prosurvival and adaptive events, including increased BCL2 expression or activation of HIF-1, have already taken place. If so, cancer cells harboring such lesions might remain sensitive to only the antiproliferative effects of mTOR inhibition.

The mTOR-regulated events that allow cells to survive in the intraluminal space are clearly separable from those that regulate cell proliferation. Specifically, mice bearing transgenes encoding both AKT and the prosurvival protein BCL2 remain sensitive to RAD001-induced inhibition of proliferation but are resistant to apoptosis. Thus, in these cells the AKT- and mTOR-induced survival activity does not result simply from first acquiring and then losing an excessive proliferation signal. The specific mechanism of apoptosis is not fully determined herein, but this pathway involves caspase-3 activation and requires an 'intact' mitochondrial pathway. These latter data are in keeping with the observation that rapamycin decreases the mitochondrial membrane potential of cells expressing activated AKT[29]. These data suggest that the therapeutic efficacy of mTOR inhibition may require the mitochondrial apoptotic pathway.

BCL2 is overexpressed in human prostate cancer[30–32] and PIN[33,34], suggesting that BCL2 expression is associated with initiation and progression of prostate cancer. Both loss of PTEN and overexpression of BCL2 have been linked to increased prostate cancer grade and the development of androgen-independent metastatic prostate cancer[30,35,36]. Indeed, in primary tumors there seems to be some correlation between PTEN loss and BCL2 overexpression[37]. Clinical trials of rapamycin derivatives RAD001 or CCI-779 are ongoing in patients with advanced prostate cancer[16,38,39], in whom *PTEN* mutation is frequent[36]. If our data are predictive of human prostate cancer sensitivity, mTOR inhibition may be less effective in advanced prostate cancers characterized by BCL2 overexpression. Phase 2 clinical trials of agents that directly or indirectly modulate BCL2 functions are also underway[40–43]. Our results provide a rationale for combination therapy with mTOR inhibitors and BCL2 inhibitors.

Finally, our data suggest that a major component of the *in vivo* transcriptional response to activation of AKT is mTOR-dependent regulation of Hif-1α. It is notable that alterations in Hif-1 activity preceded any change in the phenotype by several days, lending credence to the idea that these are primary, not secondary, events. Therefore, it is possible that the failure to confer full resistance to RAD001 by BCL2 coexpression is due to a continued need for elevated Hif-1α activity and elevated glycolytic activity. If so, a prediction is that constitutive Hif-1α activity might lead to resistance to mTOR inhibition.

Downstream of PI3K signaling, both Akt-dependent, mTOR-independent and Akt dependent, mTOR-dependent regulation of Hif-1α have been described[44,45]. In our model, Akt-dependent induction of Hif-1α activity is entirely mTOR dependent. These *in vivo* results support data suggesting that hypoxia-induced activation of Hif-1α requires mTOR activity[46,47], that insulin activates Hif-1α through an Akt- and mTOR-dependent pathway[48] and that, in the setting of loss of *Tsc2*, Hif-1α protein and mRNA levels are elevated,

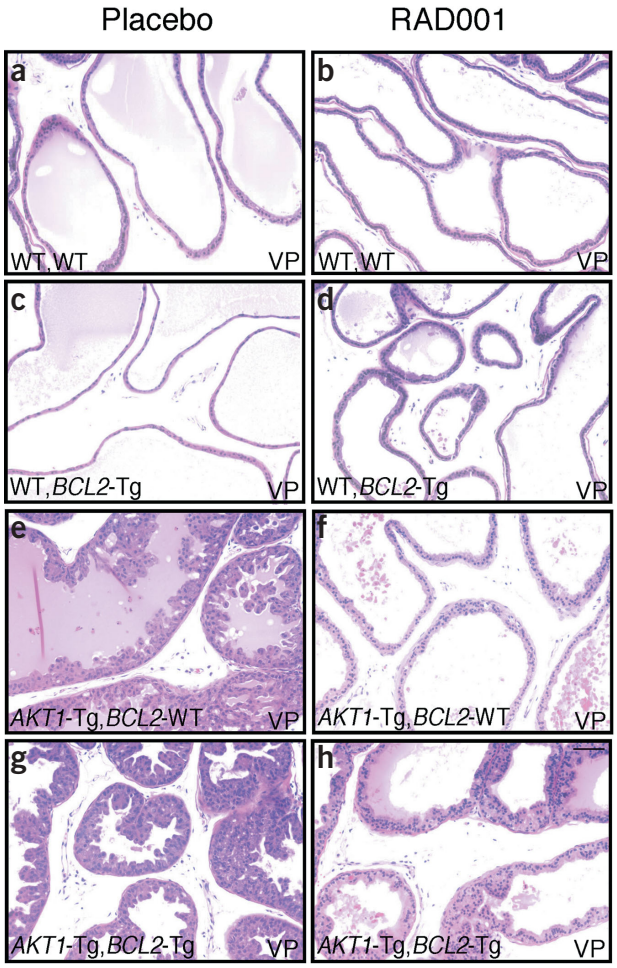

Figure 5 Complete phenotype regression after mTOR inhibition requires the mitochondrial apoptosis pathway. (**a**–**h**) Wild-type (WT, WT) (**a**,**b**), wild-type *AKT1*-Tg and transgenic *BCL2* (WT, *BCL2*-Tg) (**c**,**d**), *AKT1*-Tg, *BCL2* wild-type (*AKT1*-Tg, *BCL2*-WT) (**e**,**f**) and *AKT1*-Tg,*BCL2*-Tg (*AKT1*-Tg, *BCL2*-Tg) mice (**g**,**h**) were treated for 14 d with either placebo (**a**,**c**,**e**,**g**) or 10 mg/kg/d RAD001 (**b**,**d**,**f**,**h**) administered orally. Shown are representative H&E-stained tissue sections from the ventral prostate. Scale bar, 50 μm.

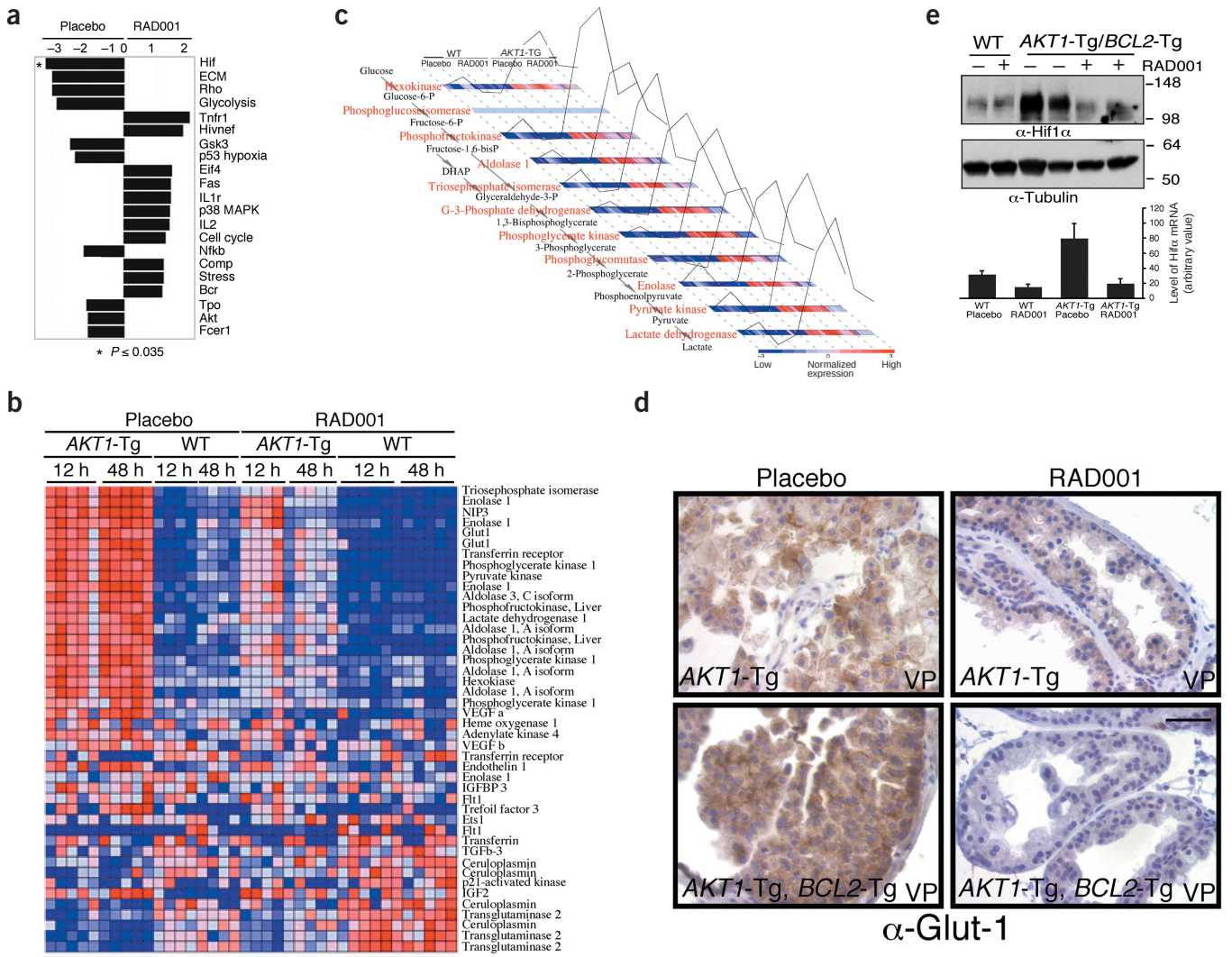

Figure 6 Expression profiles of mTOR inhibition are enriched for Hif-1α targets and glycolysis genes. (**a**) The top 21 gene sets enriched by GSEA; (–) and (+) indicate RAD001 down- or upregulation. (**b**) GSEA for 44 Hif-1α targets ranked by high expression in placebo as compared to RAD001 treatment. Expression values are represented by standard deviations above (red) or below (blue) the mean. (**c**) The mean fold expression (black line) for each glycolytic enzyme (red) is shown (substrates are in black). Expression values are also shown as in **b**. (**d**) Glut-1 immunostaining in RAD001- or placebo-treated ventral prostate (VP). Scale bar, 25 μm. (**e**) Hif-1α immunoblotting in RAD001 (+) or placebo (–) treated ventral prostate. Hif-1α mRNA expression was determined in the indicated mice after 48 h of treatment (from microarray data).

leading to upregulated expression of Hif-1α targets[49]. Elevated Hif-1α activity is, in this setting, reversed by mTOR inhibition[49]. Although the mechanism leading to mTOR-dependent elevated Hif-1α activity remains unclear, rapamycin seems to interfere with Hif-1α activation in hypoxic cells by increasing the rate of Hif-1α degradation through the oxygen-dependent domain[46]. In the *AKT1*-Tg ventral prostate, increased mTOR activity is associated with a 3.2-fold increase in the Hif-1α mRNA itself that is normalized with mTOR inhibition (**Fig. 6e**). Thus, it is likely that mTOR has both transcriptional and post-translational effects on Hif-1α.

The link between mTOR and GLUT1 induction may have immediate clinical relevance, as glucose uptake can be imaged in humans by [^{18}F]fluorodeoxyglucose positron emission tomography (FDG-PET). Thus, in patients treated with mTOR inhibitors, a rapid down-regulation of FDG-PET intensity might be reflective of mTOR inhibition (that is, pharmacodynamic response) rather than of general antitumor activity, and might thus allow for the identification of patients with mTOR-dependent tumors.

Finally, although the current clinical application to mTOR inhibition is targeted at later-stage cancers, the response of this early neoplastic disease model to RAD001 raises the possibility that inhibitors of mTOR may find application in treating early cancer lesions in humans.

METHODS

Mouse strains, genotyping and tissue preparation. Animal experiments were compliant with the guidelines of Dana-Farber Cancer Institute. The line FVB-Tg(Pbsn-Akt1)9Wrs (*AKT1*-Tg, also known as MPAKT) has been described[17]. Genotyping, prostate dissections, tissue fixation and H&E staining were carried out as described[17] (see http://research.dfci.harvard.edu/sellerslab/datasets/index.html for protocols).

© 2004 Nature Publishing Group http://www.nature.com/naturemedicine

The *BCL2*-Tg mice[20], maintained on a mixed C57BL6/FVB background, were intercrossed with *AKT1*-Tg heterozygous mice to generate F_1 offspring. Compound genotypes were obtained in the expected proportion.

Administration and measurement of RAD001. We administered 10 mg/kg/d of RAD001 (40-*O*-(2-hydroxyethyl)-rapamycin) as a microemulsion[50] (2% w/w) diluted in distilled, deionized water by oral gavage. Blood and dissected ventral prostates collected after 12 h, 24 h and 14 d of treatment were snap frozen and RAD001 concentrations determined by liquid chromatography.

Antibodies, microscopy, immunohistochemistry and immunoblot analysis. Tissue sections were hydrated, incubated for 30 min with 3% H_2O_2 in methanol at room temperature, washed with distilled, deionized water and PBS, and heated in a microwave oven to 199 °F (93 °C) in 1 mM EDTA (pH 8.0) for 25 min (antibodies to pRPS6, peIF4G, pAKT and activated caspase-3) or in 10 mM sodium citrate buffer (pH 6.0) for 30 min (antibody to Zo1), or heated in a pressure cooker in 10 mM citrate buffer (pH 6.0) for 30 min (antibody to pGSK3). Sections were blocked in 10% goat serum (30 min), incubated with antibodies to Akt (pS473; 1:400), pGSK3 (pS21/9; 1:25), pRPS6 (pS235/236), peIF4G (pS1108; 1:400; Cell Signaling), Glut1 (1:400; Alpha Diagnostic) and BrdU (1:100; BD Pharmingen) in 1% BSA (12 h at 4 °C), washed with PBS, incubated with secondary antibody (1:200; 30 min) and detected with the ABC kit (Vector).

Protein extracts and immunoblots were prepared as described[17]. Antibodies to phospho-Akt-S473, phospho-GSK3-S21/9, phospho-eIF4G-S1108, phospho-S6 S235/236 (Cell Signaling), human BCL2 (6C8; BD PharMingen), Hif-1α and α-tubulin (B-5-1-2; Sigma) were used at 1:1,000.

For confocal microscopy, sections were blocked in immunofluorescence buffer (IFB) (130 mM NaCl, 7 mM Na2HPO4, 3.5 mM NaH2PO4, 7.7 mM NaN3, 0.1% BSA, 0.2% Triton X-100, 0.05% Tween 20) with 10% goat serum and 20 mg/ml goat anti-mouse F(ab¢)2) for 90 min. Antibodies to pAkt (pS473; 1:200), activated caspase-3 (Asp175; 1:200) and Zo1 (1:400) were incubated overnight at room temperature in IFB. After washing in IFB, slides were incubated with Alexa-Fluor–conjugated anti-rabbit antibody (Molecular Probes) in IFB containing 10% goat serum for 60 min, washed three times with IFB, incubated for 15 min with DAPI (0.5 ng/ml in PBS; Roche) and mounted with Prolong (Molecular Probes). Confocal analysis (Pinh 1.75) was carried out using an Inverted Confocal Laser Scanning Microscope (Carl Zeiss).

TUNEL assay. Paraformaldehyde-fixed tissue sections were deparaffinized in xylene, rehydrated in ethanol and incubated with proteinase K (0.02 mg/ml) for 20 min at room temperature (21–23°), and TUNEL staining was carried out using the Fluorescein-FragEL kit (Oncogene Research Products) per the manufacturer's instructions. TUNEL-positive luminal epithelial cells were counted in all ducts, and the number of apoptotic epithelial cells per 100 ducts was calculated.

Expression analysis. Biotin-labeled cRNA prepared from 15 µg total RNA was fragmented and hybridized to oligonucleotide microarrays (430A, Affymetrix)[17]. CEL files, generated by GeneChip, were scaled to the median intensity array based on the mean value of all genes. Before analysis, genes with minimal variation (less than fivefold difference or an absolute difference of <50 between any two samples) or those outside the thresholds of 16,000 and 10 were excluded.

Candidate genes regulated by mTOR were identified using an idealized gene profile (placebo wild type 12 h and 48 h = 0, RAD001 wild type 12 h = –5, RAD001 wild type 48 h = –10, placebo *AKT1*-Tg 12 h and 48 h = 24, RAD001 *AKT1*-Tg 12 h = 12, and RAD001 *AKT1*-Tg 48 h = 0), and correlating gene expression with this ideal profile was determined using the Pearson coefficient. Permutation of the ideal profile labels was used to determine if the correlation was greater than expected by chance alone; 571 unique genes or expressed sequence tags passed permutation testing.

GSEA comparing RAD001- and placebo-treated samples (n = 9 and 10) was done using described methods and 192 previously defined gene-pathway sets[21] or a curated list of Hif-1 targets[22]. Pathways were ranked according to the significance of enrichment, and the validation mode measure of significance was used to identify pathways of greatest enrichment. For curated Hif-1 targets, enrichment was tested for RAD001 versus placebo treatment, for *AKT1*-Tg versus wild-type placebo-treated prostates, and for all placebo versus all RAD001-treated samples. Significance was tested by comparing the observed enrichment with the enrichment seen in data sets in which sample labels were randomly permuted (n = 1000).

Statistical analysis. Analysis of variance was used to test for differences in the percent apoptotic cells or BrdU incorporation between RAD001- and placebo-treated mice. The Wilcoxon rank-sum statistic was used to test for differences in the number of apoptotic cells by treatment and genotype. Student's t-test was used to test for differences in cell size by treatment.

ACKNOWLEDGMENTS

We thank M.A. Brown and W.G. Kaelin for critical comments; J. Shim, N. Bhattacharya, A. Thorner and S. Luo for technical assistance; and J. Pouyssegur for the Hif-1 antibody. This work was supported the Linda and Arthur Gelb Center for Translational Research, by the National Cancer Institute (PO1CA89021), by CaPCURE, by the Damon-Runyon Cancer Research Foundation (W.R.S.) and by a Career Development Award from the DF/HCC SPORE in Prostate Cancer (P.K.M.).

Note: Supplementary information is available on the Nature Medicine website.

COMPETING INTEREST STATEMENT

The authors declare competing financial interests (see the *Nature Medicine* website for details).

Received 19 January; accepted 28 April 2004
Published online at http://www.nature.com/naturemedicine/

1. Maehama, T. & Dixon, J.E. The tumor suppressor, PTEN/MMAC1, dephosphorylates the lipid second messenger, phosphatidylinositol 3,4,5-trisphosphate. *J. Biol. Chem.* **273**, 13375–13378 (1998).
2. del Peso, L., Gonzalez-Garcia, M., Page, C., Herrera, R. & Nunez, G. Interleukin-3-induced phosphorylation of BAD through the protein kinase Akt. *Science* **278**, 687–689 (1997).
3. Kops, G.J. *et al.* Direct control of the Forkhead transcription factor AFX by protein kinase B. *Nature* **398**, 630–634 (1999).
4. Nakamura, N. *et al.* Forkhead transcription factors are critical effectors of cell death and cell cycle arrest downstream of PTEN. *Mol. Cell. Biol.* **20**, 8969–8982 (2000).
5. Cross, D.A., Alessi, D.R., Cohen, P., Andjelkovich, M. & Hemmings, B.A. Inhibition of glycogen synthase kinase-3 by insulin mediated by protein kinase B. *Nature* **378**, 785–789 (1995).
6. Goberdhan, D.C., Paricio, N., Goodman, E.C., Mlodzik, M. & Wilson, C. Drosophila tumor suppressor PTEN controls cell size and number by antagonizing the Chico/PI3-kinase signaling pathway. *Genes Dev.* **13**, 3244–3258 (1999).
7. Oldham, S., Montagne, J., Radimerski, T., Thomas, G. & Hafen, E. Genetic and biochemical characterization of dTOR, the Drosophila homolog of the target of rapamycin. *Genes Dev.* **14**, 2689–2694 (2000).
8. Neshat, M.S. *et al.* Enhanced sensitivity of PTEN-deficient tumors to inhibition of FRAP/mTOR. *Proc. Natl. Acad. Sci. USA* **98**, 10314–10319 (2001).
9. Podsypanina, K. *et al.* An inhibitor of mTOR reduces neoplasia and normalizes p70/S6 kinase activity in $Pten^{+/-}$ mice. *Proc. Natl. Acad. Sci. USA* **98**, 10320–10325 (2001).
10. Aoki, M., Blazek, E. & Vogt, P.K. A role of the kinase mTOR in cellular transformation induced by the oncoproteins P3k and Akt. *Proc. Natl. Acad. Sci. USA* **98**, 136–141 (2001).
11. Manning, B.D., Tee, A.R., Logsdon, M.N., Blenis, J. & Cantley, L.C. Identification of the tuberous sclerosis complex-2 tumor suppressor gene product tuberin as a target of the phosphoinositide 3-kinase/akt pathway. *Mol. Cell* **10**, 151–162 (2002).
12. Gao, X. *et al.* Tsc tumour suppressor proteins antagonize amino-acid-TOR signalling. *Nat. Cell Biol.* **4**, 699–704 (2002).
13. Gao, X. & Pan, D. TSC1 and TSC2 tumor suppressors antagonize insulin signaling in cell growth. *Genes Dev.* **15**, 1383–192 (2001).
14. Potter, C.J., Huang, H. & Xu, T. Drosophila Tsc1 functions with Tsc2 to antagonize insulin signaling in regulating cell growth, cell proliferation, and organ size. *Cell* **105**, 357–368 (2001).
15. Tee, A.R., Manning, B.D., Roux, P.P., Cantley, L.C. & Blenis, J. Tuberous sclerosis complex gene products, Tuberin and Hamartin, control mTOR signaling by acting as a GTPase-activating protein complex toward Rheb. *Curr. Biol.* **13**, 1259–1268 (2003).
16. Huang, S. & Houghton, P.J. Inhibitors of mammalian target of rapamycin as novel antitumor agents: from bench to clinic. *Curr. Opin. Invest. Drugs* **3**, 295–304 (2002).
17. Majumder, P.K. *et al.* Prostate intraepithelial neoplasia induced by prostate restricted Akt activation: the MPAKT model. *Proc. Natl. Acad. Sci. USA* **100**, 7841–7846 (2003).

© 2004 Nature Publishing Group http://www.nature.com/naturemedicine

18. Nashan, B. Early clinical experience with a novel rapamycin derivative. *Ther. Drug Monit.* **24**, 53–58 (2002).
19. Raught, B. *et al.* Serum-stimulated, rapamycin-sensitive phosphorylation sites in the eukaryotic translation initiation factor 4GI. *EMBO J.* **19**, 434–444 (2000).
20. Bruckheimer, E.M. *et al.* The impact of bcl-2 expression and bax deficiency on prostate homeostasis *in vivo*. *Oncogene* **19**, 2404–2412 (2000).
21. Mootha, V.K. *et al.* PGC-1α-responsive genes involved in oxidative phosphorylation are coordinately downregulated in human diabetes. *Nat. Genet.* **34**, 267–273 (2003).
22. Semenza, G. Signal transduction to hypoxia-inducible factor 1. *Biochem. Pharmacol.* **64**, 993–998 (2002).
23. Sellers, W.R. & Sawyers, C.A. Somatic genetics of prostate cancer: oncogenes and Tumor Suppressors. in *Prostate Cancer Principles and Practice* (ed. Kantoff, P.) (Lippincott Williams & Wilkins, Philadelphia, USA, 2002).
24. Samuels, Y. *et al.* High frequency of mutations of the *PIK3CA* gene in human cancers. *Science* **304**, 554 (2004).
25. Shayesteh, L. *et al. PIK3CA* is implicated as an oncogene in ovarian cancer. *Nat. Genet.* **21**, 99–102 (1999).
26. Debnath, J. *et al.* The role of apoptosis in creating and maintaining luminal space within normal and oncogene-expressing mammary acini. *Cell* **111**, 29–40 (2002).
27. Debnath, J., Walker, S.J. & Brugge, J.S. Akt activation disrupts mammary acinar architecture and enhances proliferation in an mTOR-dependent manner. *J. Cell. Biol.* **163**, 315–326 (2003).
28. Wendel, H.G. *et al.* Survival signalling by Akt and eIF4E in oncogenesis and cancer therapy. *Nature* **428**, 332–337 (2004).
29. Edinger, A.L. & Thompson, C.B. Akt maintains cell size and survival by increasing mTOR-dependent nutrient uptake. *Mol. Biol. Cell* **13**, 2276–2288 (2002).
30. McDonnell, T.J. *et al.* Expression of the protooncogene bcl-2 in the prostate and its association with emergence of androgen-independent prostate cancer. *Cancer Res.* **52**, 6940–6944 (1992).
31. Furuya, Y., Krajewski, S., Epstein, J.I., Reed, J.C. & Isaacs, J.T. Expression of bcl-2 and the progression of human and rodent prostatic cancers. *Clin. Cancer Res.* **2**, 389–398 (1996).
32. Krajewska, M. *et al.* Immunohistochemical analysis of bcl-2, bax, bcl-X, and mcl-1 expression in prostate cancers. *Am. J. Pathol.* **148**, 1567–1576 (1996).
33. Colombel, M. *et al.* Detection of the apoptosis-suppressing oncoprotein bc1-2 in hormone-refractory human prostate cancers. *Am. J. Pathol.* **143**, 390–400 (1993).
34. Baltaci, S., Orhan, D., Ozer, G., Tolunay, O. & Gogous, O. Bcl-2 proto-oncogene expression in low- and high-grade prostatic intraepithelial neoplasia. *BJU Int.* **85**, 155–159 (2000).
35. McMenamin, M.E. *et al.* Loss of PTEN expression in paraffin-embedded primary prostate cancer correlates with high Gleason score and advanced stage. *Cancer Res.* **59**, 4291–4296 (1999).
36. Suzuki, H. *et al.* Interfocal heterogeneity of PTEN/MMAC1 gene alterations in multiple metastatic prostate cancer tissues. *Cancer Res.* **58**, 204–209 (1998).
37. Huang, H. *et al.* PTEN induces chemosensitivity in PTEN-mutated prostate cancer cells by suppression of Bcl-2 expression. *J. Biol. Chem.* **276**, 38830–38836 (2001).
38. Mita, M.M., Mita, A. & Rowinsky, E.K. Mammalian target of rapamycin: a new molecular target for breast cancer. *Clin. Breast Cancer* **4**, 126–137 (2003).
39. Hidalgo, M. & Rowinsky, E.K. The rapamycin-sensitive signal transduction pathway as a target for cancer therapy. *Oncogene* **19**, 6680–6686 (2000).
40. Chi, K.N. *et al.* A phase I dose-finding study of combined treatment with an antisense Bcl-2 oligonucleotide (Genasense) and mitoxantrone in patients with metastatic hormone-refractory prostate cancer. *Clin. Cancer Res.* **7**, 3920–3927 (2001).
41. Morris, M.J. *et al.* Phase I trial of BCL-2 antisense oligonucleotide (G3139) administered by continuous intravenous infusion in patients with advanced cancer. *Clin. Cancer Res.* **8**, 679–683 (2002).
42. DiPaola, R.S. *et al.* Phase I clinical and pharmacologic study of 13-cis-retinoic acid, interferon alfa, and paclitaxel in patients with prostate cancer and other advanced malignancies. *J. Clin. Oncol.* **17**, 2213–2218 (1999).
43. Friedland, D. *et al.* A phase II trial of docetaxel (Taxotere) in hormone-refractory prostate cancer: correlation of antitumor effect to phosphorylation of Bcl-2. *Semin. Oncol.* **26**, 19–23 (1999).
44. Semenza, G.L. Targeting HIF-1 for cancer therapy. *Nat. Rev. Cancer* **3**, 721–732 (2003).
45. Abraham, R.T. mTOR as a positive regulator of tumor cell responses to hypoxia. *Curr. Top. Microbiol. Immunol.* **279**, 299–319 (2004).
46. Hudson, C.C. *et al.* Regulation of hypoxia-inducible factor 1α expression and function by the mammalian target of rapamycin. *Mol. Cell. Biol.* **22**, 7004–7014 (2002).
47. Zhong, H. *et al.* Modulation of hypoxia-inducible factor 1α expression by the epidermal growth factor/phosphatidylinositol 3-kinase/PTEN/AKT/FRAP pathway in human prostate cancer cells: implications for tumor angiogenesis and therapeutics. *Cancer Res.* **60**, 1541–1545 (2000).
48. Treins, C., Giorgetti-Peraldi, S., Murdaca, J., Semenza, G.L. & Van Obberghen, E. Insulin stimulates hypoxia-inducible factor 1 through a phosphatidylinositol 3-kinase/target of rapamycin-dependent signaling pathway. *J. Biol. Chem.* **277**, 27975–27981 (2002).
49. Brugarolas, J.B., Vazquez, F., Reddy, A., Sellers, W.R. & Kaelin, W.G., Jr. TSC2 regulates VEGF through mTOR-dependent and -independent pathways. *Cancer Cell* **4**, 147–158 (2003).
50. Taesch, S. & Niese, D. Safety and tolerability of a new oral formulation of cyclosporin A, Sandimmun Neoral, in renal transplant patients. *Transpl. Int.* **7** (suppl. 1), S263–S266 (1994).

© 2004 Nature Publishing Group http://www.nature.com/naturemedicine